Supporting information for

Tin and lead phosphanido complexes: reactivity with chalcogens

Eric C. Y. Tam,[†] David C. Apperley,[‡] J. David Smith,[†] Martyn P. Coles[†,§] and J. Robin Fulton[,†,§]*

† Department of Chemistry, University of Sussex, Falmer, Brighton BN1 9QJ.

‡ Department of Chemistry, University of Durham, South Road, Durham, U.K.

§ School of Chemical and Physical Sciences, Victoria University of Wellington, P.O. Box 600, Wellington 6012, New Zealand

Fig S1	Abbreviated ORTEP diagram for [(BDI)PbSePCy$_2$] (**2-Pb-Cy-Se**)	S3
Fig S2	Abbreviated ORTEP diagram for [(BDI)PbSeP(Se)Cy$_2$] (**4-Pb-Cy-Se$_2$**)	S3
Fig S3	Abbreviated ORTEP diagram for [(BDI)SnSP(S)Cy$_2$] (**4-Sn-Cy-S$_2$**)	S3
Fig S4	Solid-state ^{31}P{^{1}H} NMR spectrum of [(BDI)SnSePCy$_2$] (**2-Sn-Cy-Se**)	S4
Fig S5	Solid-state ^{77}Se{^{1}H} NMR spectrum of [(BDI)SnSePCy$_2$] (**2-Sn-Cy-Se**)	S4
Fig S6	Solid-state ^{31}P{^{1}H} NMR spectrum of [(BDI)SnSeP(Se)Cy$_2$] (**4-Sn-Cy-Se$_2$**)	S5
Fig S7	^{1}H NMR spectrum of [(BDI)PbSePCy$_2$] (**2-Pb-Cy-Se**)	S5
Fig S8	^{13}C{^{1}H} NMR spectrum of [(BDI)PbSePCy$_2$] (**2-Pb-Cy-Se**)	S6
Fig S9	^{31}P{^{1}H} NMR spectrum of [(BDI)PbSePCy$_2$] (**2-Pb-Cy-Se**)	S6
Fig S10	^{77}Se NMR spectrum of [(BDI)PbSePCy$_2$] (**2-Pb-Cy-Se**)	S7

Fig S11	^{207}Pb NMR spectrum of [(BDI)PbSePCy$_2$] (**2-Pb-Cy-Se**)	S7
Fig S12	^{1}H NMR spectrum of [(BDI)SnSP(S)Cy$_2$] (**4-Sn-Cy-S$_2$**)	S8
Fig S13	^{13}C{^{1}H} NMR spectrum of [(BDI)SnSP(S)Cy$_2$] (**4-Sn-Cy-S$_2$**)	S8
Fig S14	^{31}P{^{1}H} NMR spectrum of [(BDI)SnSP(S)Cy$_2$] (**4-Sn-Cy-S$_2$**)	S9
Fig S15	^{119}Sn NMR spectrum of [(BDI)SnSP(S)Cy$_2$] (**4-Sn-Cy-S$_2$**)	S9
Fig S16	^{1}H NMR spectrum of [(BDI)PbSP(S)Cy$_2$] (**4-Pb-Cy-S$_2$**)	S10
Fig S17	^{13}C{^{1}H} NMR spectrum of [(BDI)PbSP(S)Cy$_2$] (**4-Pb-Cy-S$_2$**)	S10
Fig S18	^{31}P{^{1}H} NMR spectrum of [(BDI)PbSP(S)Cy$_2$] (**4-Pb-Cy-S$_2$**)	S11
Fig S19	^{207}Pb NMR spectrum of [(BDI)PbSP(S)Cy$_2$] (**4-Pb-Cy-S$_2$**)	S11
Fig S10	^{1}H NMR spectrum of [(BDI)Sn(S/Se)P(S/Se)Cy$_2$] (**4-Sn-Cy-S/Se**)	S12
Fig S21	^{13}C{^{1}H} NMR spectrum of [(BDI)Sn(S/Se)P(S/Se)Cy$_2$] (**4-Sn-Cy-S/Se)**	S12
Fig S22	^{31}P{^{1}H} NMR spectrum of [(BDI)Sn(S/Se)P(S/Se)Cy$_2$] (**4-Sn-Cy-S/Se)**	S13
Fig S23	^{77}Se NMR spectrum of [(BDI)Sn(S/Se)P(S/Se)Cy$_2$] (**4-Sn-Cy-S/Se**)	S13
Fig S24	^{119}Sn NMR spectrum of [(BDI)Sn(S/Se)P(S/Se)Cy$_2$] (**4-Sn-Cy-S/Se**)	S14
Table S1	Data collection parameters for **2-Sn-Cy-Se**, **2-Pb-Cy-Se**, **4-Sn-Cy-Se$_2$** and **4-Pb-Cy-Se$_2$**	S15
Table S2	Data collection parameters for **4-Sn-Cy-S$_2$**, **4-Pb-Cy-S$_2$** and **6**	S16
Fig S25	ORTEP diagram for [(BDI)SnSePCy$_2$] (**2-Sn-Cy-Se**)	S17
Fig S26	ORTEP diagram for [(BDI)PbSePCy$_2$] (**2-Pb-Cy-Se**)	S17
Fig S27	ORTEP diagram for [(BDI)SnSeP(Se)Cy$_2$] (**4-Sn-Cy-Se$_2$**)	S18
Fig S28	ORTEP diagram for [(BDI)PbSeP(Se)Cy$_2$] (**4-Pb-Cy-Se$_2$**)	S18
Fig S29	ORTEP diagram for [(BDI)SnSP(S)Cy$_2$] (**4-Sn-Cy-S$_2$**)	S19
Fig S30	ORTEP diagram for [(BDI)PbSP(S)Cy$_2$] (**4-Pb-Cy-S$_2$**)	S19
Fig S28	ORTEP diagram for [(BDI)SnSeSiMe$_3$] (**6**)	S20

Figure S1. ORTEP diagram of lead(II) dicyclohexylphosphinoselenoite, **2-Pb-Cy-Se**. H atoms omitted and BDI C atoms minimized for clarity. The ellipsoid probability is shown at 30%.

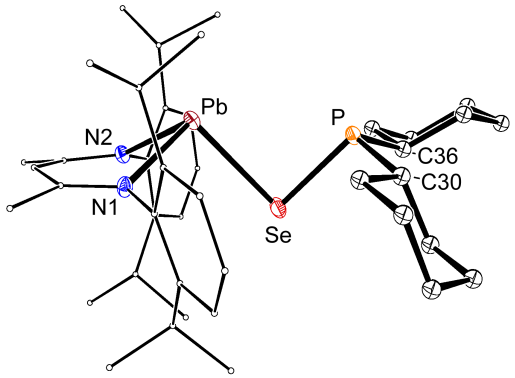

Figure S2. ORTEP diagram of lead(II) dicyclohexylphosphinodiselenoate, **4-Pb-Cy-Se$_2$**. H atoms omitted and BDI C atoms minimized for clarity. The ellipsoid probability is shown at 30%.

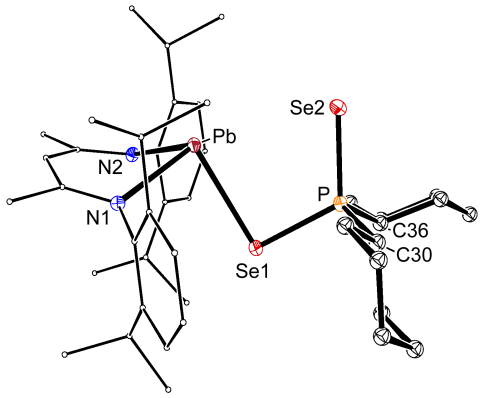

Figure S3. ORTEP diagram of tin(II) dicyclohexylphosphinodiselenoate, **4-Sn-Cy-S$_2$**. H atoms omitted and BDI C atoms minimized for clarity. The ellipsoid probability is shown at 30%.

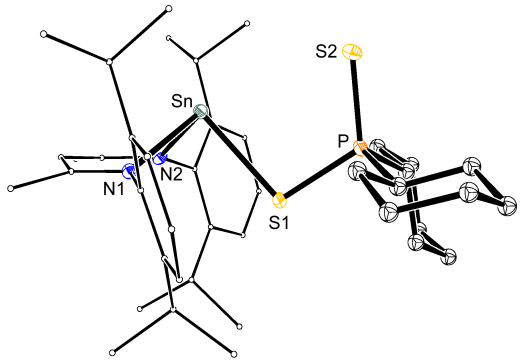

Figure S4. Solid-state $^{31}P\{^{1}H\}$ NMR spectrum of [(BDI)SnSePCy$_2$] (**2-Sn-Cy-Se**).

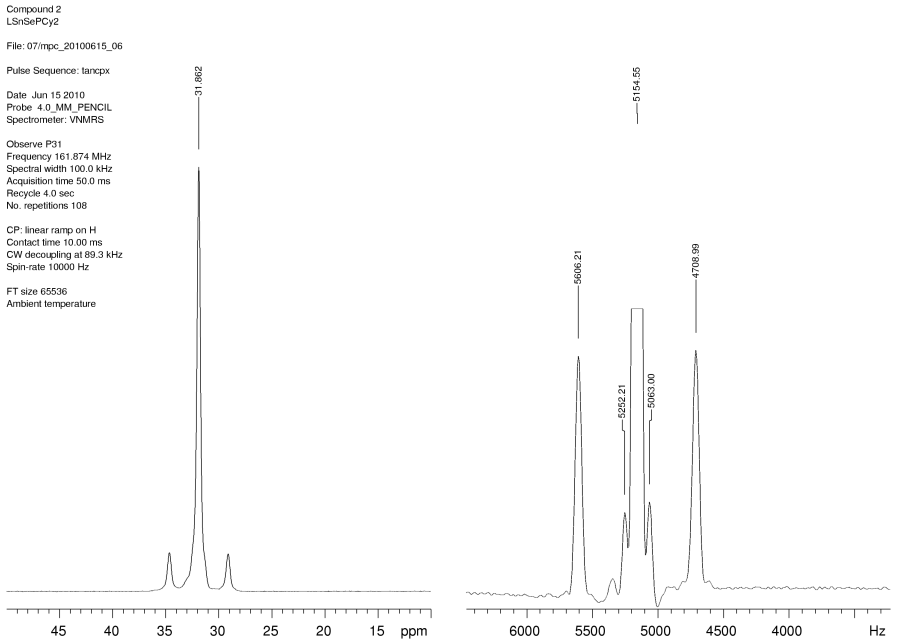

Figure S5. Solid-state $^{77}Se\{^{1}H\}$ NMR spectrum of [(BDI)SnSePCy$_2$] (**2-Sn-Cy-Se**)

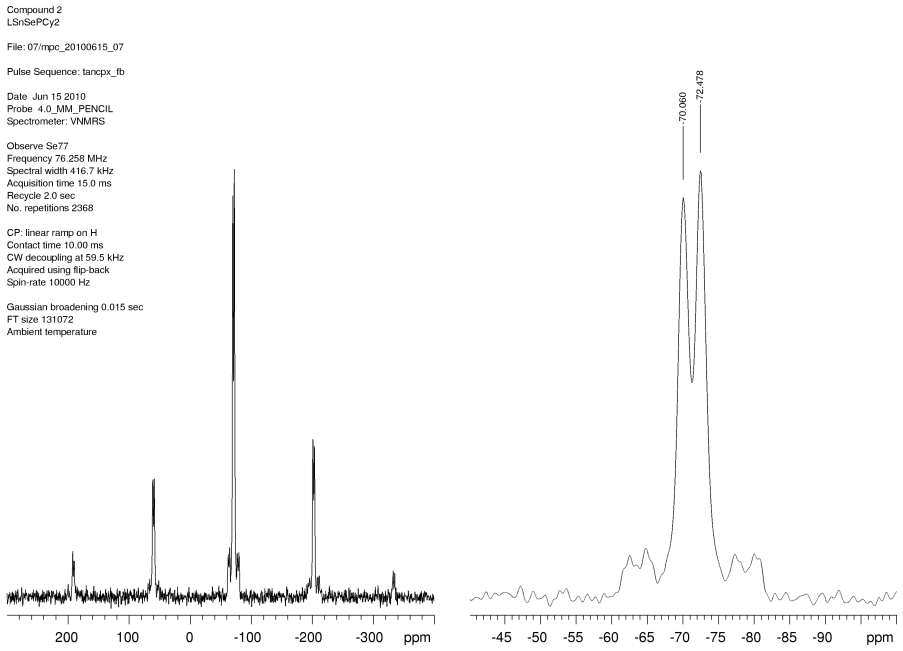

Figure S6. Solid-state $^{31}P\{^{1}H\}$ NMR spectrum of [(BDI)SnSeP(Se)Cy_2] (**4-Sn-Cy-Se$_2$**)

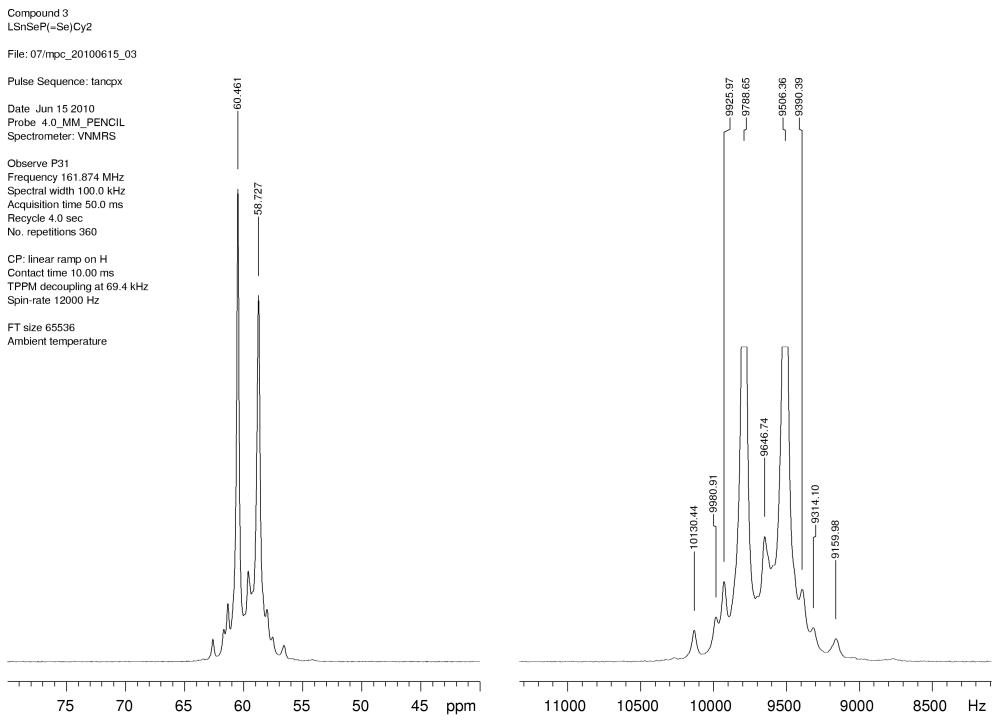

Figure S7. ^{1}H NMR spectrum of [(BDI)PbSePCy$_2$] (**2-Pb-Cy-Se**)

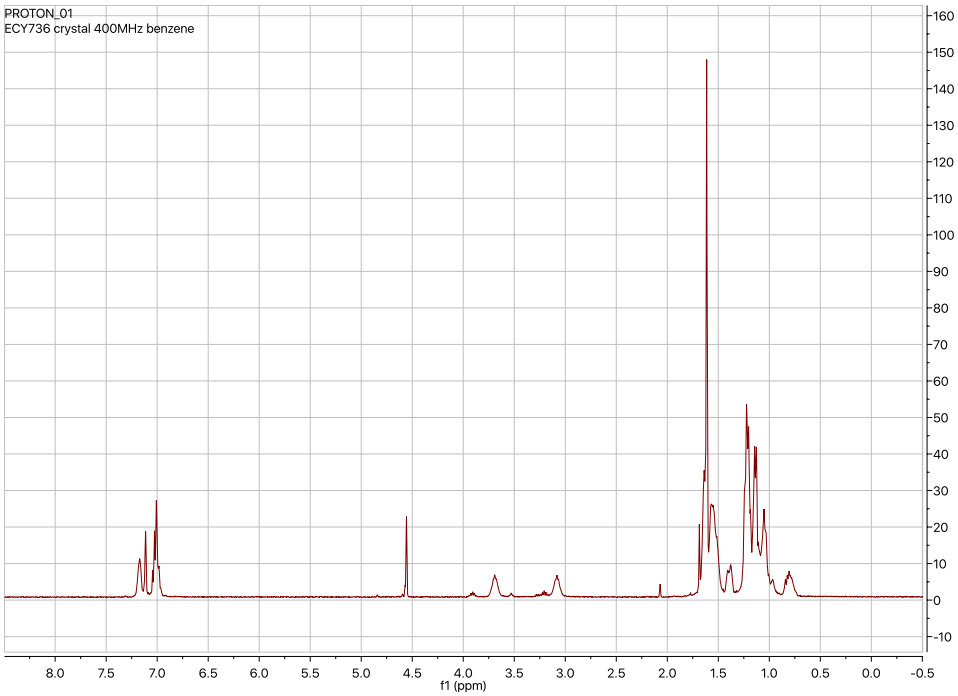

Figure S8. $^{13}C\{^{1}H\}$ NMR spectrum of [(BDI)PbSePCy$_2$] (**2-Pb-Cy-Se**)

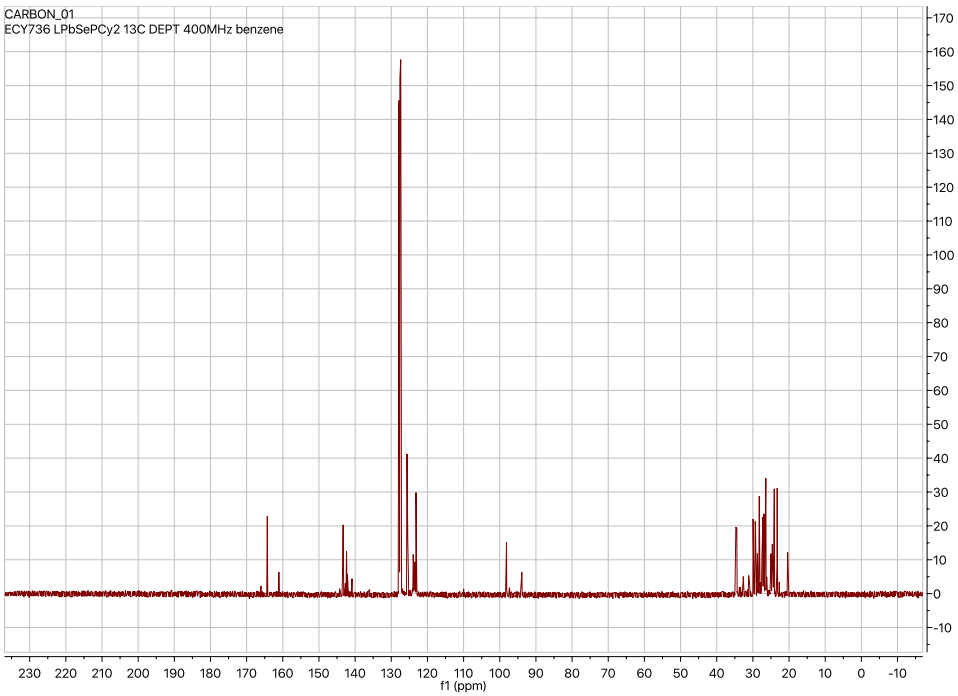

Figure S9. $^{31}P\{^{1}H\}$ NMR spectrum of [(BDI)PbSePCy$_2$] (**2-Pb-Cy-Se**)

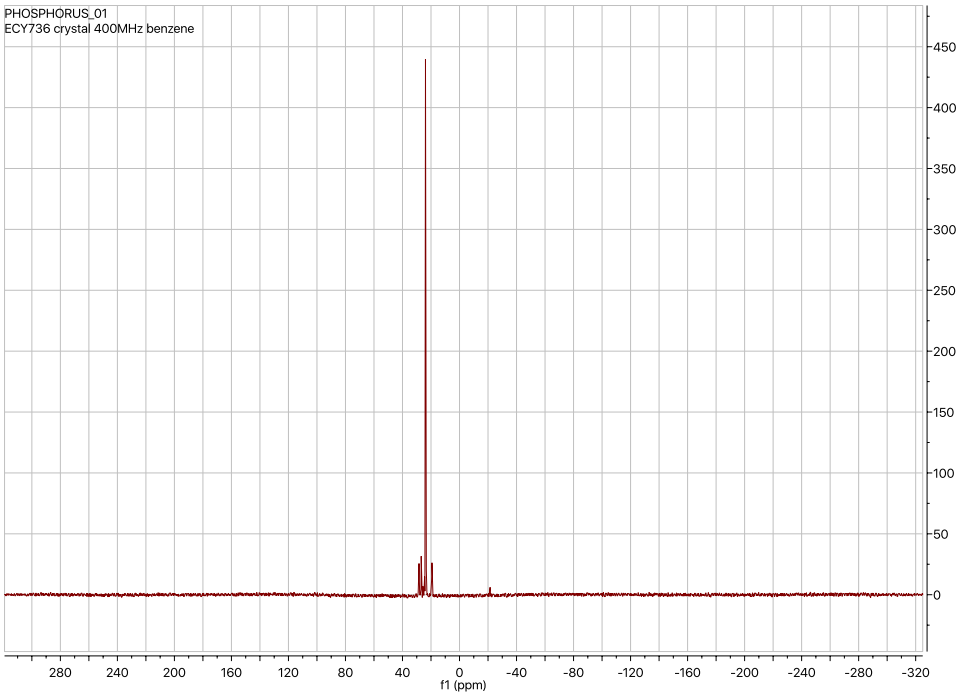

Figure S10. ^{77}Se NMR spectrum of [(BDI)PbSePCy$_2$] (**2-Pb-Cy-Se**)

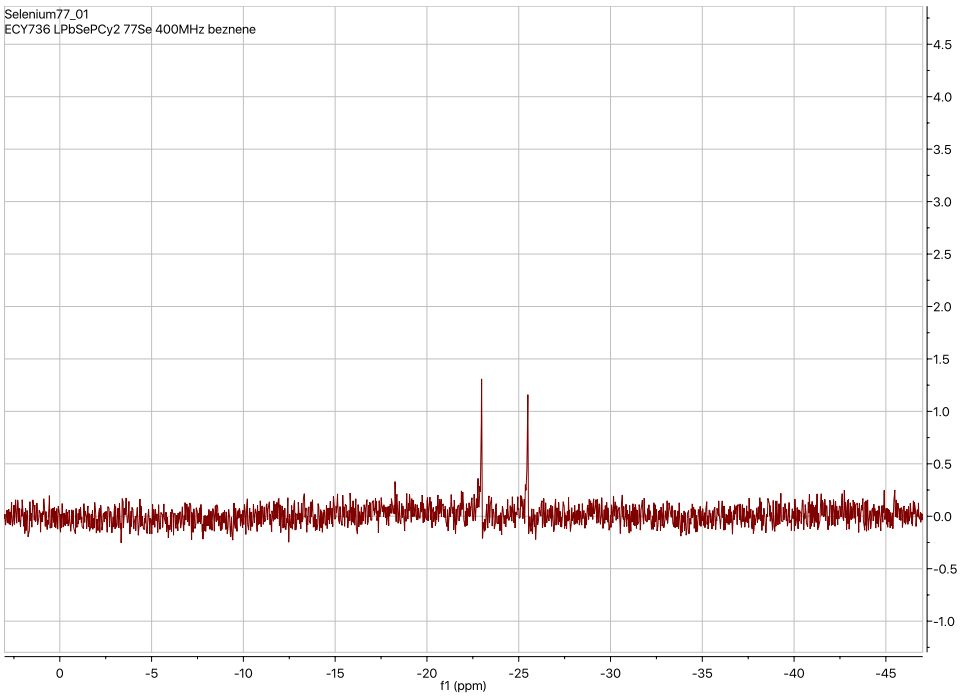

Figure S11. ^{207}Pb NMR spectrum of [(BDI)PbSePCy$_2$] (**2-Pb-Cy-Se**)

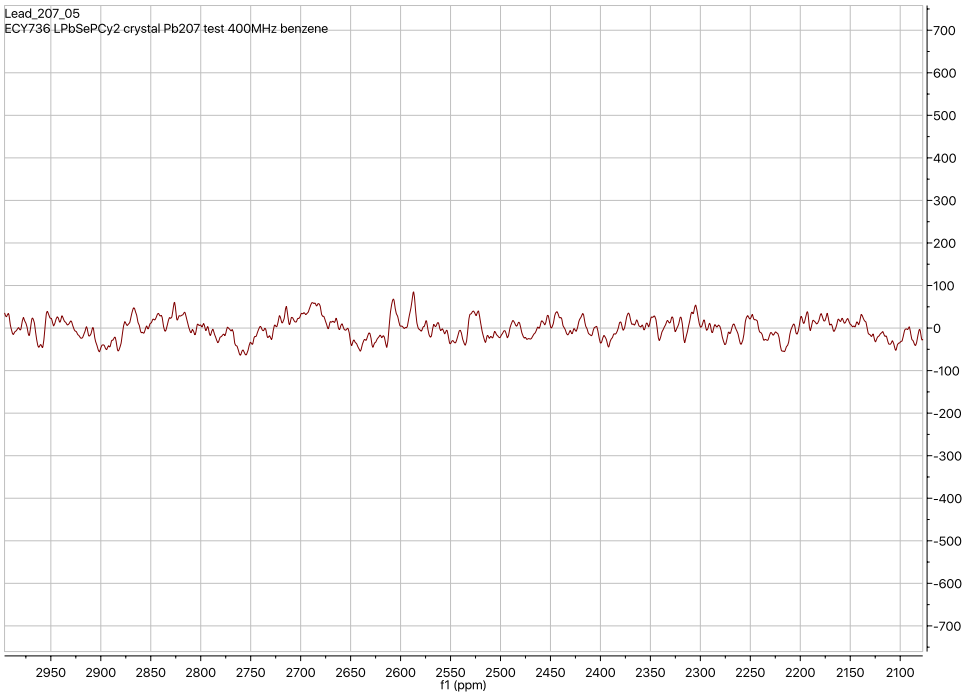

Figure S12. ^{1}H NMR spectrum of [(BDI)SnSP(S)Cy$_2$] (**4-Sn-Cy-S**)

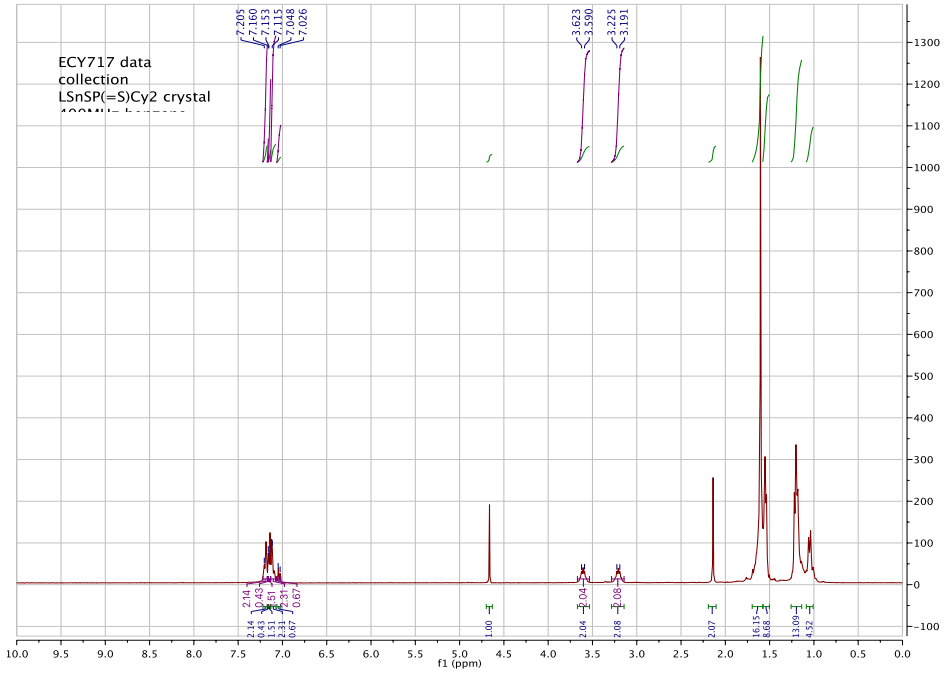

Figure S13. ^{13}C{^{1}H} NMR spectrum of [(BDI)SnSP(S)Cy$_2$] (**4-Sn-Cy-S**)

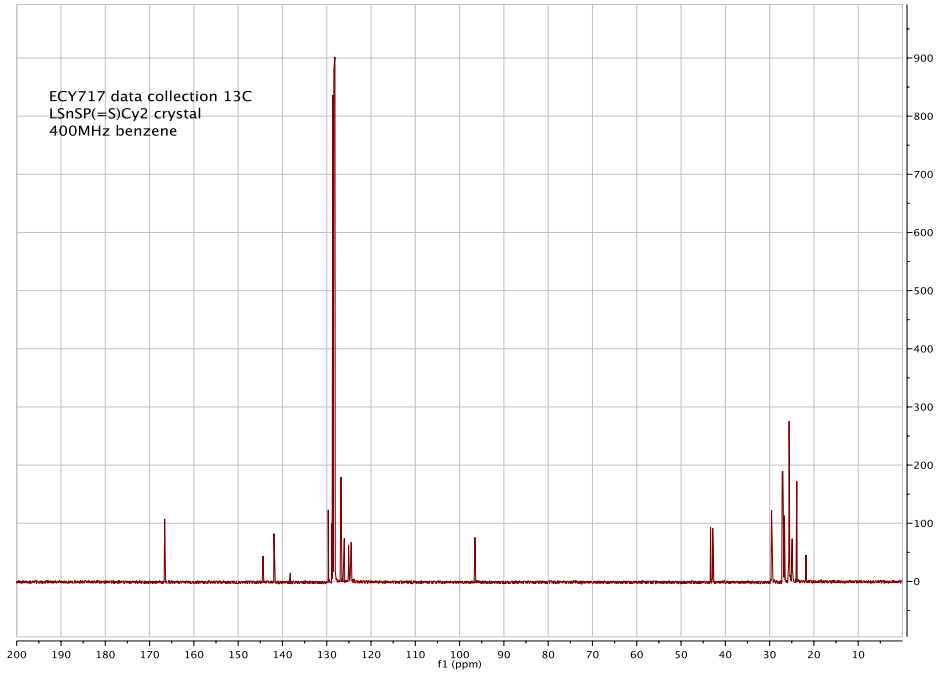

Figure S14. $^{31}P\{^{1}H\}$ NMR spectrum of [(BDI)SnSP(S)Cy_2] (**4-Sn-Cy-S**)

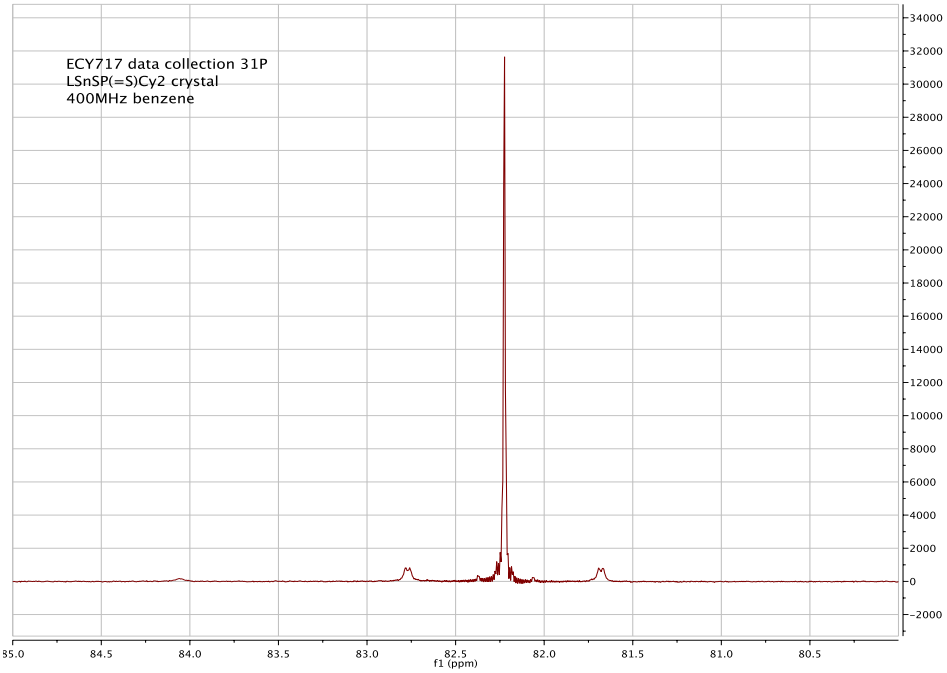

Figure S15. ^{119}Sn NMR spectrum of [(BDI)SnSP(S)Cy_2] (**4-Sn-Cy-S**)

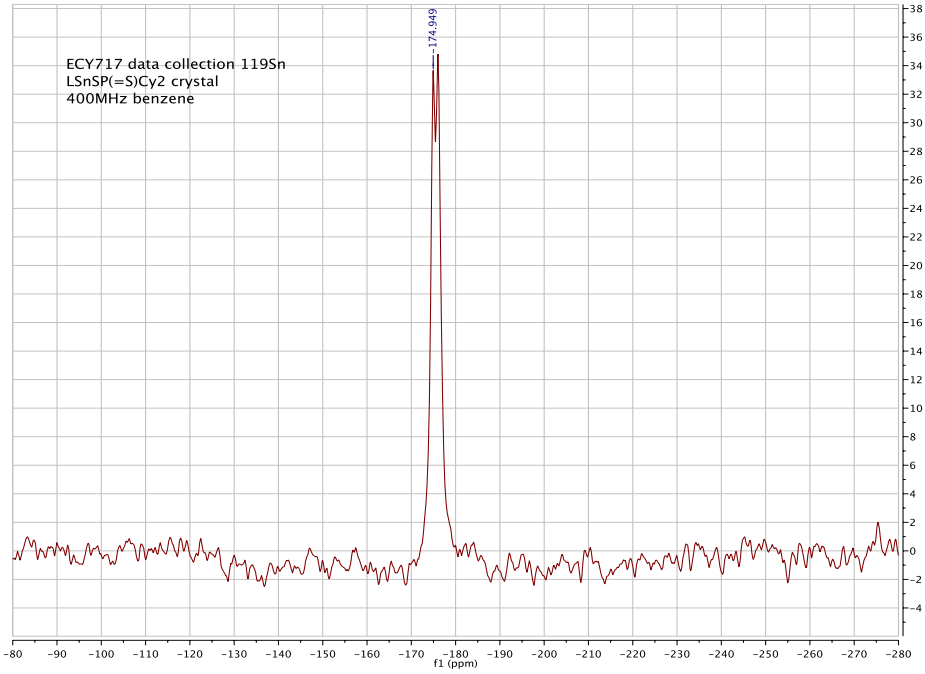

Figure S16. ^{1}H NMR spectrum of [(BDI)PbSP(S)Cy$_2$] (**4-Pb-Cy-S**)

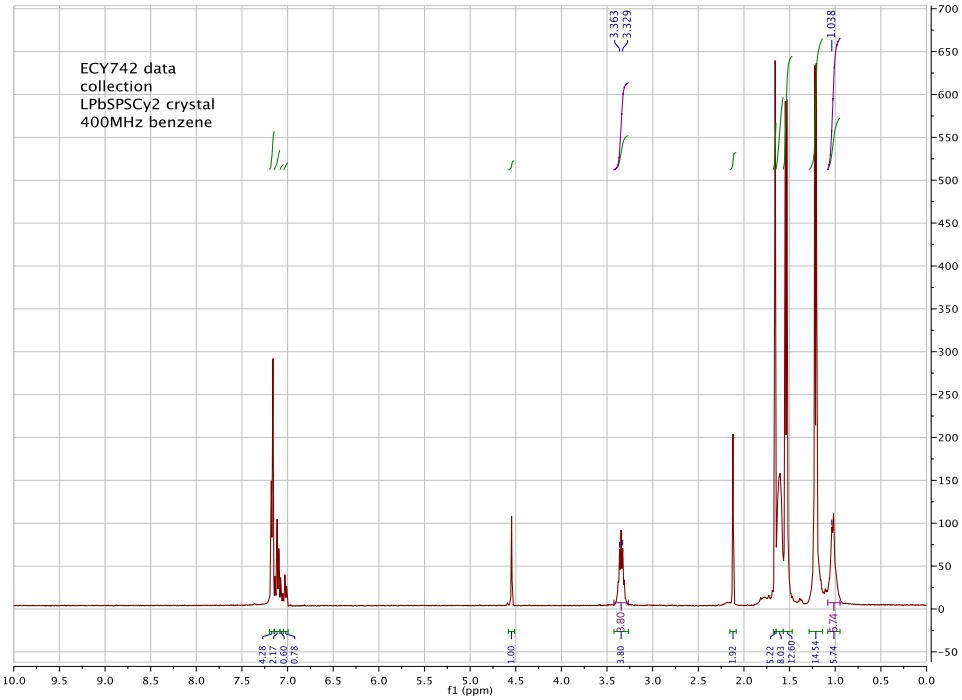

Figure S17. ^{13}C{^{1}H} NMR spectrum of [(BDI)PbSP(S)Cy$_2$] (**4-Pb-Cy-S**)

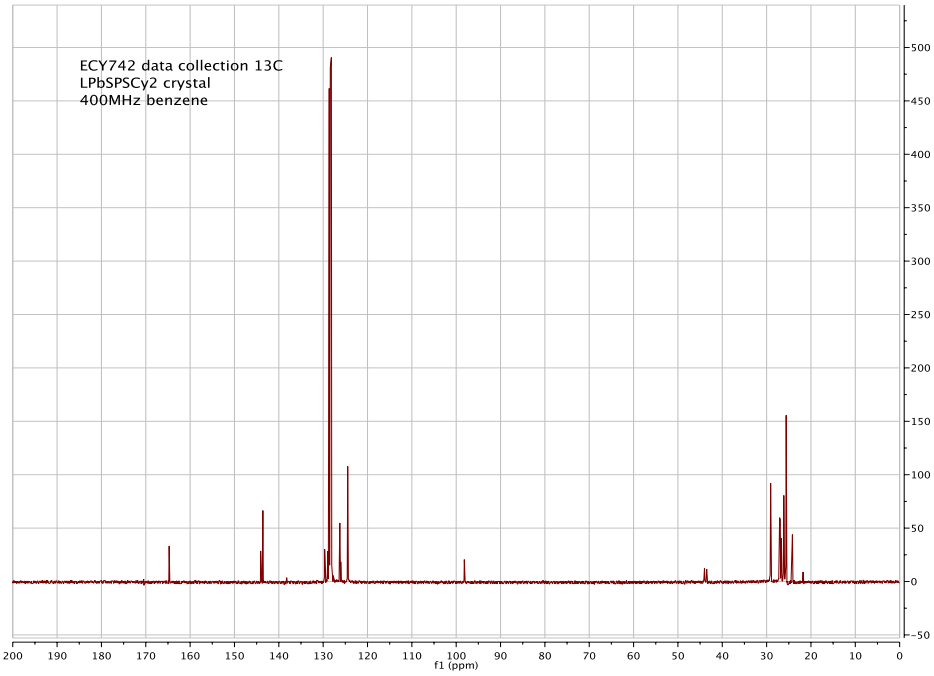

Figure S18. $^{31}P\{^{1}H\}$ NMR spectrum of [(BDI)PbSP(S)Cy_2] (**4-Pb-Cy-S**)

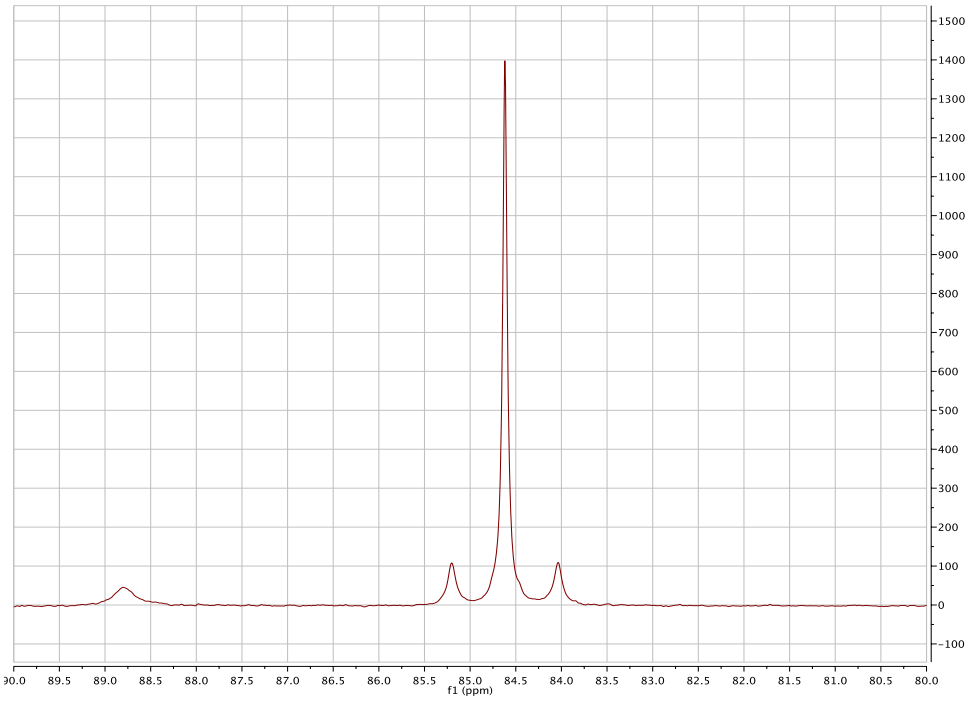

Figure S19. ^{207}Pb NMR spectrum of [(BDI)PbSP(S)Cy_2] (**4-Pb-Cy-S**)

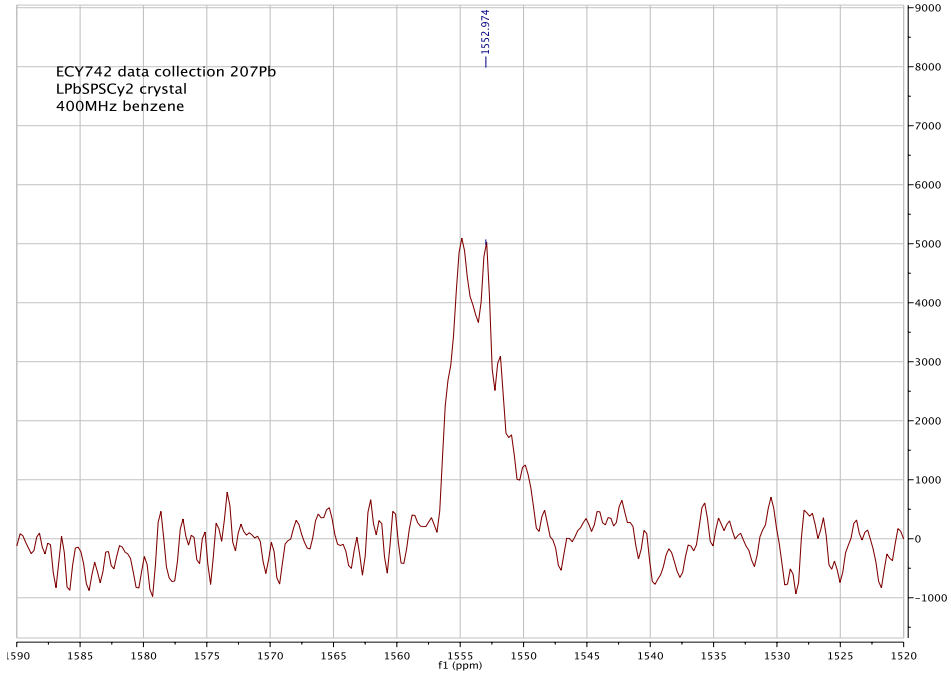

Figure S20. ^{1}H NMR spectrum of [(BDI)Sn(S/Se)P(S/Se)Cy$_2$] (**4-Sn-Cy-S/Se**)

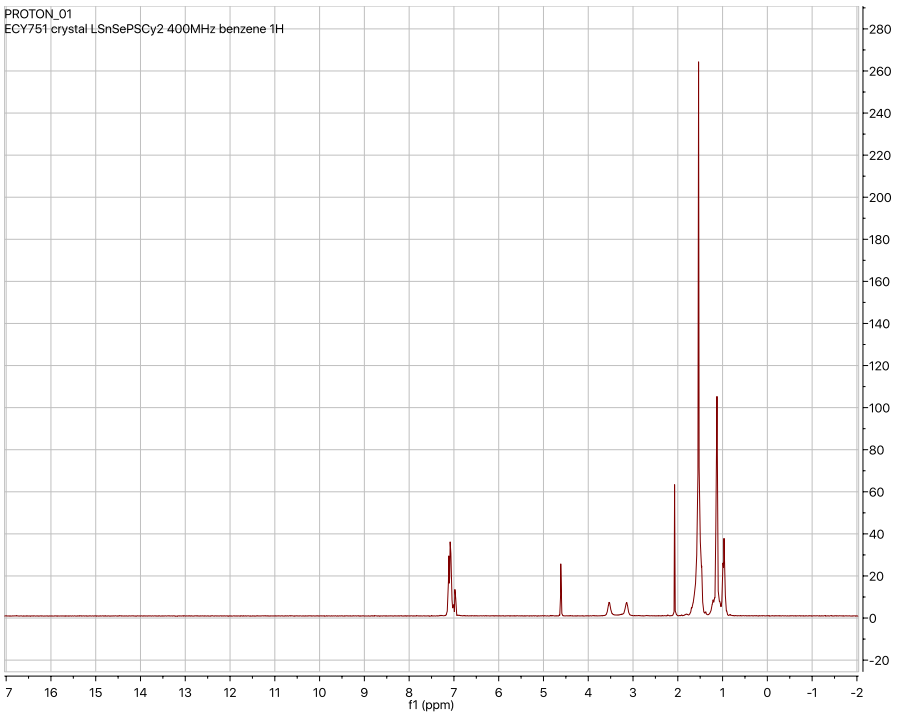

Figure S21. ^{13}C{^{1}H} NMR spectrum of [(BDI)Sn(S/Se)P(S/Se)Cy$_2$] (**4-Sn-Cy-S/Se**)

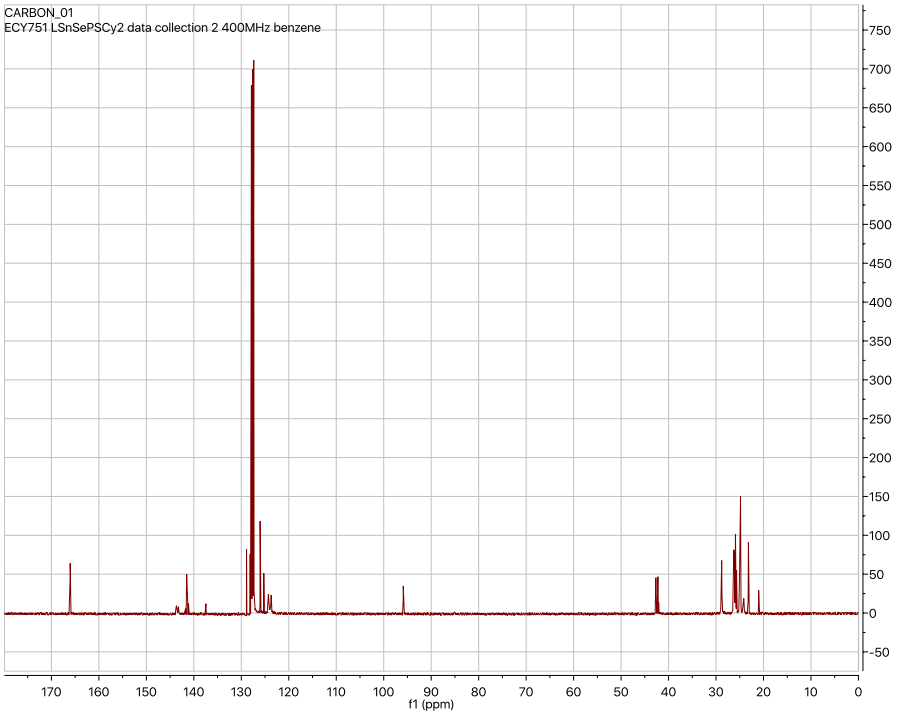

Figure S22. $^{31}P\{^{1}H\}$ NMR spectrum of [(BDI)Sn(S/Se)P(S/Se)Cy_2] (**4-Sn-Cy-S/Se**)

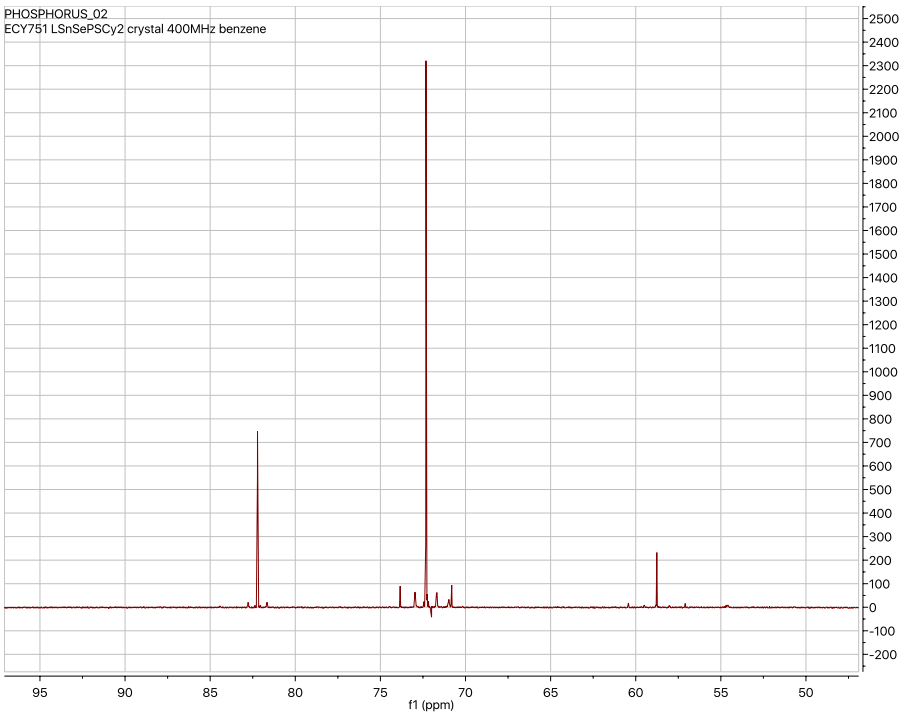

Figure S23. ^{77}Se NMR spectrum of [(BDI)Sn(S/Se)P(S/Se)Cy_2] (**4-Sn-Cy-S/Se**)

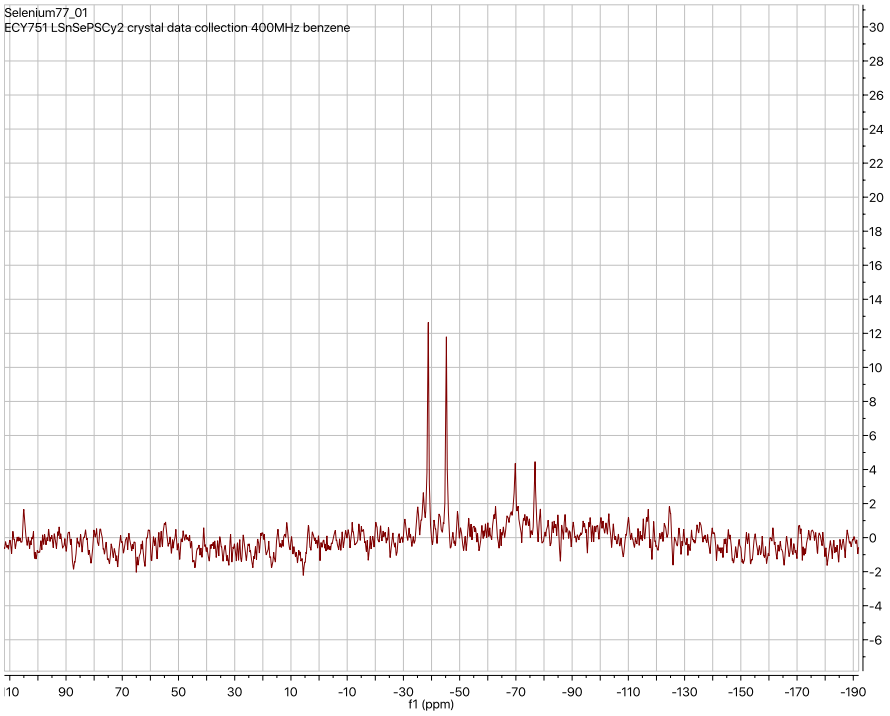

Figure S24. ^{119}Sn NMR spectrum of [(BDI)Sn(S/Se)P(S/Se)Cy$_2$] (**4-Sn-Cy-S/Se**)

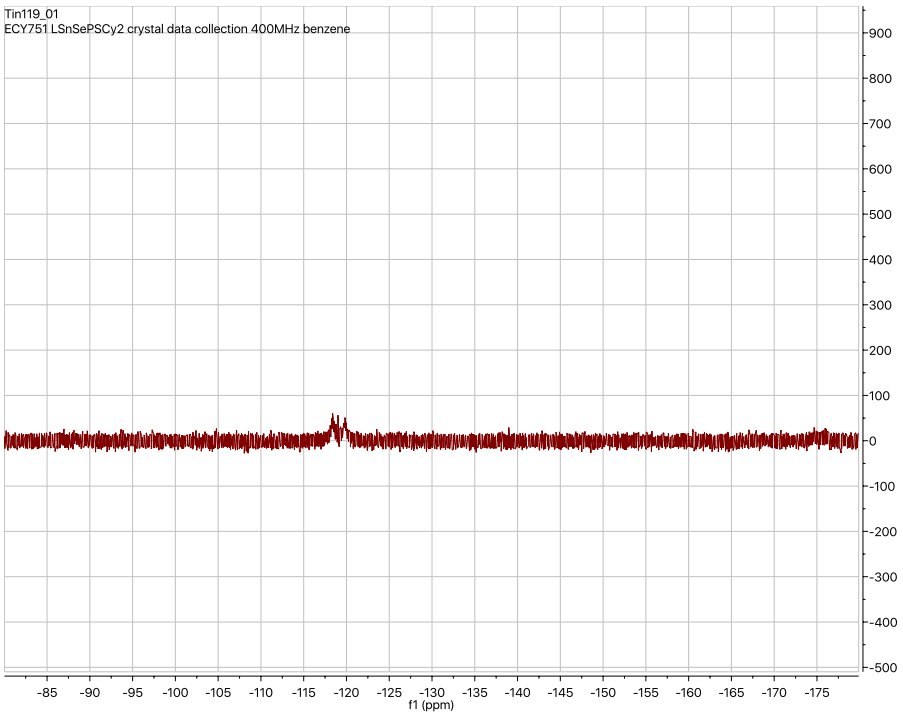

Table S1 Crystal structure and refinement data for **2-Sn-Cy-Se**, **2-Pb-Cy-Se**, **4-Sn-Cy-Se** and **4-Pb-Cy-Se**.

	(BDI)Sn(SePCy$_2$) (**2-Sn-Cy-Se**)	(BDI)Pb(SePCy$_2$) (**2-Pb-Cy-Se**)	[(BDI)SnSeP(Se)Cy$_2$] • toluene (**4-Sn-Cy-Se**)	[(BDI)PbSeP(Se)Cy$_2$] • toluene (**4-Pb-Cy-Se**)
Formula	$C_{41}H_{63}N_2PSeSn$	$C_{41}H_{63}N_2PSePb$	$C_{41}H_{63}N_2PSe_2Sn$, C_7H_8	$C_{41}H_{63}N_2PSe_2Pb$, C_7H_8
Formula weight	812.55	901.05	983.65	1072.15
Temperature (K)	173(2)	120(2)	173(2)	173(2)
Wavelength (Å)	0.71073	0.71073	0.71073	0.71073
Crystal size (mm)	0.21 x 0.10 x 0.08	0.16 x 0.14 x 0.05	0.18 x 0.11 x 0.09	0.19 x 0.08 x 0.08
Crystal system	Triclinic	Triclinic	Orthorhombic	Orthorhombic
Space group	$P\bar{1}$ (No.2)	$P\bar{1}$ (No.2)	$P\,2_1\,2_1\,2_1$ (No.19)	$P\,2_1\,2_1\,2_1$ (No.19)
a (Å)	12.1426(2)	12.1375(2)	10.3830(1)	10.3409(1)
b (Å)	12.5330(3)	12.5352(3)	15.4846(2)	15.5230(2)
c (Å)	14.2375(3)	14.2900(3)	29.7411(4)	29.7674(3)
α (°)	91.844(1)	92.391(1)	90	90
β (°)	97.593(1)	97.371(1)	90	90
γ (°)	108.807(1)	108.474(1)	90	90
V (Å^3)	2026.58(7)	2037.23(7)	4781.67	4778.32(9)
Z	2	2	4	4
D_c (Mg m^{-3})	1.33	1.47	1.37	1.49
Absorption coefficient (mm^{-1})	1.60	5.10	2.12	5.12
θ range for data collection (°)	3.43 to 27.11	3.43 to 27.11	3.56 to 27.10	3.56 to 27.11
Reflections collected	37018	37354	78235	67740
Independent reflections	8928 [R(int) = 0.051]	8987 [R(int) = 0.058]	10512 [R(int) = 0.079]	10498 [R(int) = 0.066]
Reflections [$I > 2\sigma(I)$]	7625	7806	8993	9794
Data/restraints/parameters	8928 / 0 / 417	8987 / 0 / 417	10512 / 0 / 454	10498 / 0 / 489
Goodness-of-fit on F^2	1.032	0.973	1.022	1.031
Final R indices [$I > 2\sigma(I)$]	R1 = 0.030, wR2 = 0.064	R1 = 0.030, wR2 = 0.063	R1 = 0.037, wR2 = 0.074	R1 = 0.026, wR2 = 0.049
R indices (all data)	R1 = 0.040, wR22 = 0.068	R1 = 0.040, wR22 = 0.66	R1 = 0.050, wR22 = 0.078	R1 = 0.031, wR22 = 0.052
Largest diff. peak/hole (e Å^{-3})	0.42 and -0.62	0.66 and -1.00	1.174 and -0.473	0.65 and -0.43

Table S1 Crystal structure and refinement data for **4-Sn-Cy-S**, **4-Pb-Cy-S** and **6**.

	[(BDI)SnSP(S)Cy_2] • toluene (**4-Sn-Cy-S**)	[(BDI)PbSP(S)Cy_2] • toluene (**4-Pb-Cy-S**)	[(BDI)SnSeSiMe_3] • ½ toluene (**6**)[a]
Formula	$C_{41}H_{63}N_2PS_2Sn$, C_7H_8	$C_{41}H_{63}N_2PS_2Pb$, C_7H_8	$C_{32}H_{50}N_2SiSeSn$, 0.5 C_7H_8
Formula weight	889.85	978.35	734.55
Temperature (K)	120(2)	173(2)	173(2)
Wavelength (Å)	0.71073	0.71073	0.71073
Crystal size (mm)	0.20 x 0.10 x 0.07	0.1 x 0.08 x 0.08	0.20 x 0.08 x 0.08
Crystal system	Monoclinic	Orthorhombic	Triclinic
Space group	$P\,2_1/c$ (No.14)	$P\,2_1\,2_1\,2_1$ (No.19)	$P\bar{1}$ (No.2)
a (Å)	13.1888(2)	10.1944(1)	10.6632(13)
b (Å)	18.2309(2)	15.4698(2)	11.9105(13)
c (Å)	20.4088(3)	29.9406(4)	15.2531(18)
α (°)	90	90	101.567(8)
β (°)	103.817(1)	90	93.519(6)
γ (°)	90	90	105.196(7)
V (Å^3)	4765.17(11)	4721.79	1818.2(4)
Z	4	4	2
D_c (Mg m^{-3})	1.24	1.38	1.34
Absorption coefficient (mm^{-1})	0.69	3.73	1.76
θ range for data collection (°)	3.51 to 27.10	3.58 to 26.73	3.44 to 26.02
Reflections collected	74584	74892	23354
Independent reflections	10472 [R(int) = 0.062]	10004 [R(int) = 0.095]	6805 [R(int) = 0.045]
Reflections [$I > 2\sigma(I)$]	8789	8799	5942
Data/restraints/parameters	10472 / 0 / 489	10004 / 0 / 439	6805 / 7 / 375
Goodness-of-fit on F^2	1.018	1.087	1.064
Final R indices [$I > 2\sigma(I)$]	R1 = 0.032, wR2 = 0.071	R1 = 0.035, wR2 = 0.066	R1 = 0.040, wR2 = 0.088
R indices (all data)	R1 = 0.045, wR22 = 0.76	R1 = 0.047, wR22 = 0.069	R1 = 0.049, wR22 = 0.092
Largest diff. peak/hole (e Å^{-3})	0.47 and -0.68	0.934 and -0.708	0.87 and -1.00

[a] Diffraction was weak; one of the ^{i}Pr groups is disordered; the toluene was refined as a rigid body at half occupancy with carbon atoms isotropic

Figure S25. ORTEP diagram for [(BDI)SnSePCy$_2$] (**2-Sn-Cy-Se**).

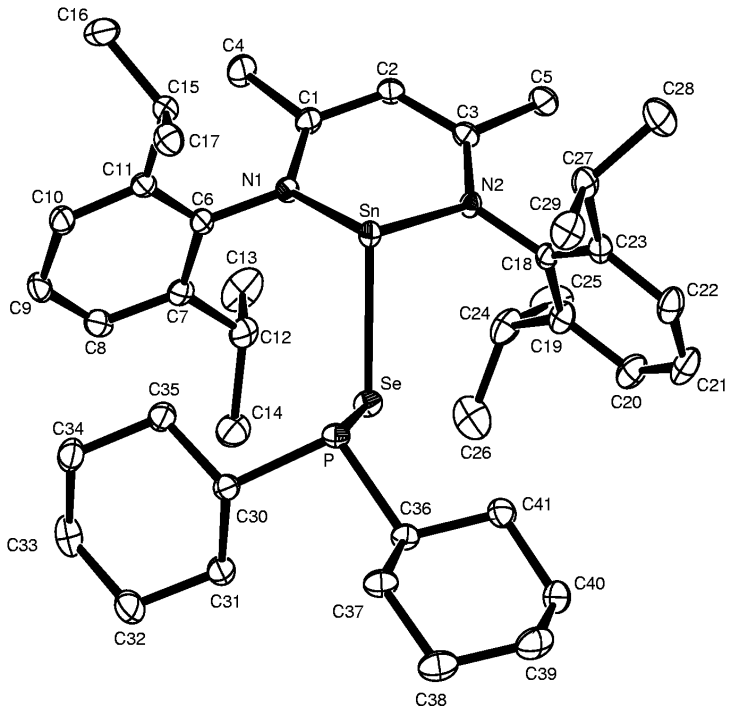

Figure S26. ORTEP diagram for [(BDI)PbSePCy$_2$] (**2-Pb-Cy-Se**).

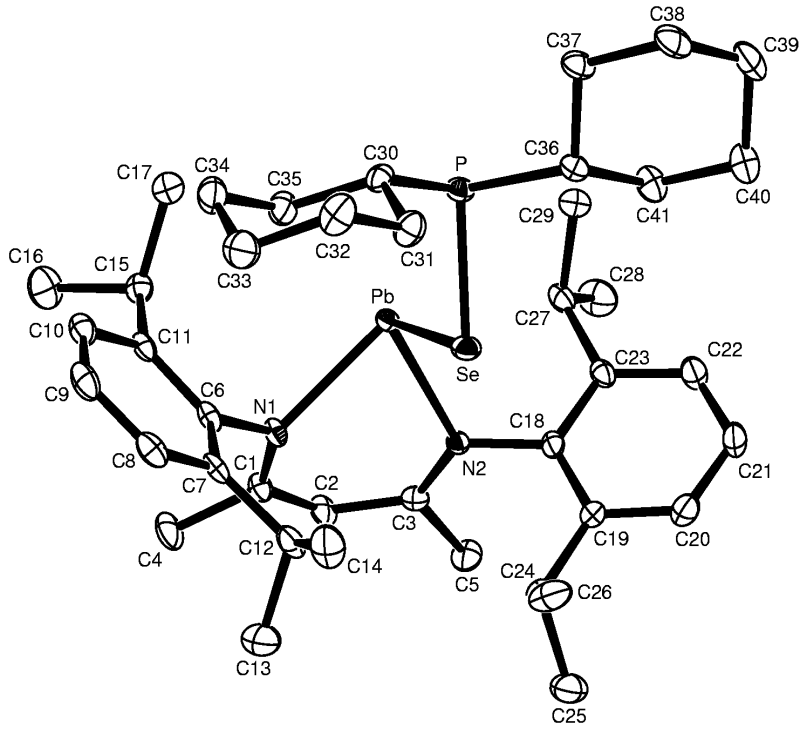

Figure S27. ORTEP diagram for [(BDI)SnSeP(Se)Cy_2] (**4-Sn-Cy-Se**).

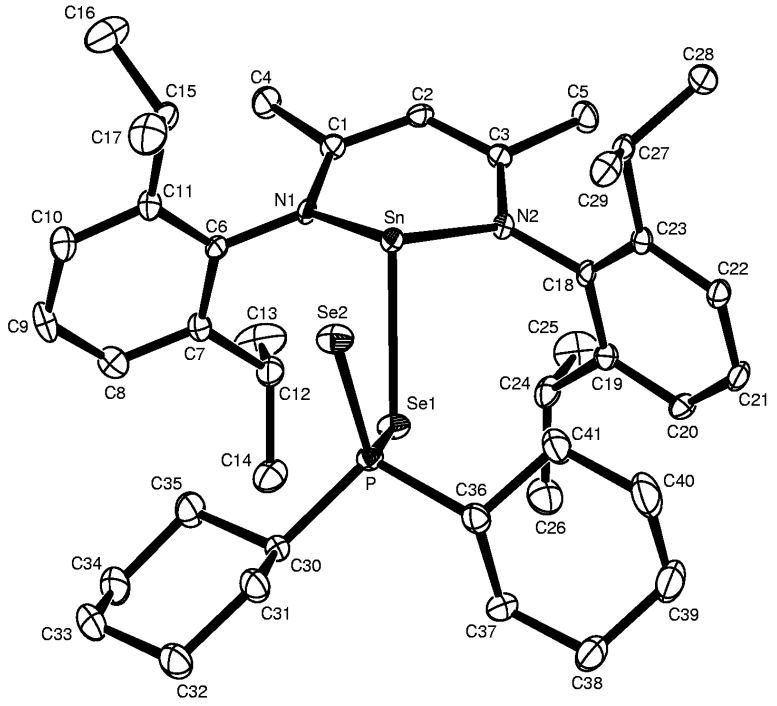

Figure S28. ORTEP diagram for [(BDI)PbSeP(Se)Cy_2] (**4-Pb-Cy-Se**).

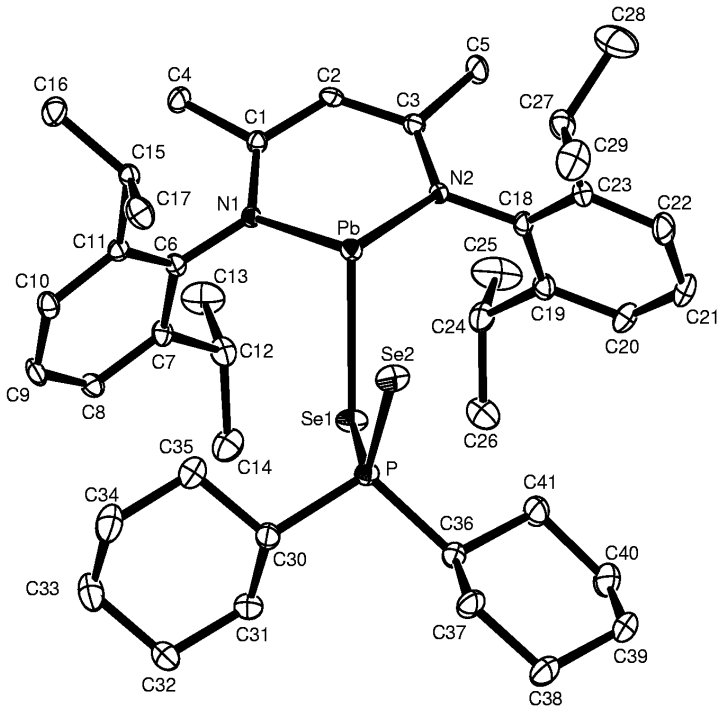

Figure S29. ORTEP diagram for [(BDI)SnSP(S)Cy_2] (**4-Sn-Cy-S**).

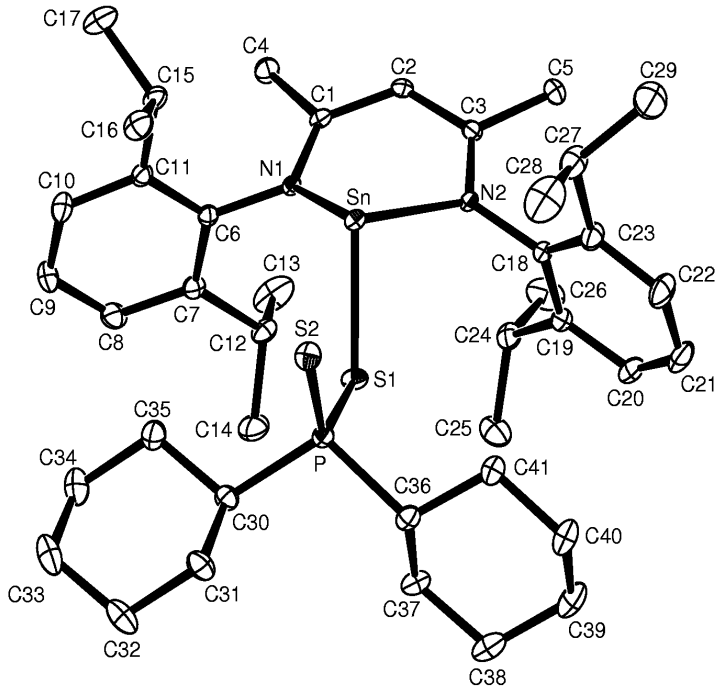

Figure S30. ORTEP diagram for [(BDI)PbSP(S)Cy_2] (**4-Pb-Cy-S**).

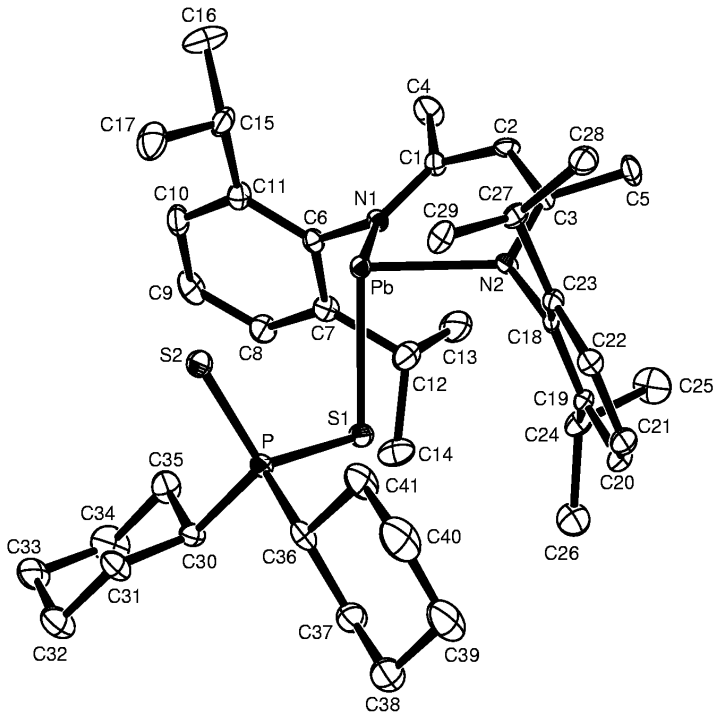
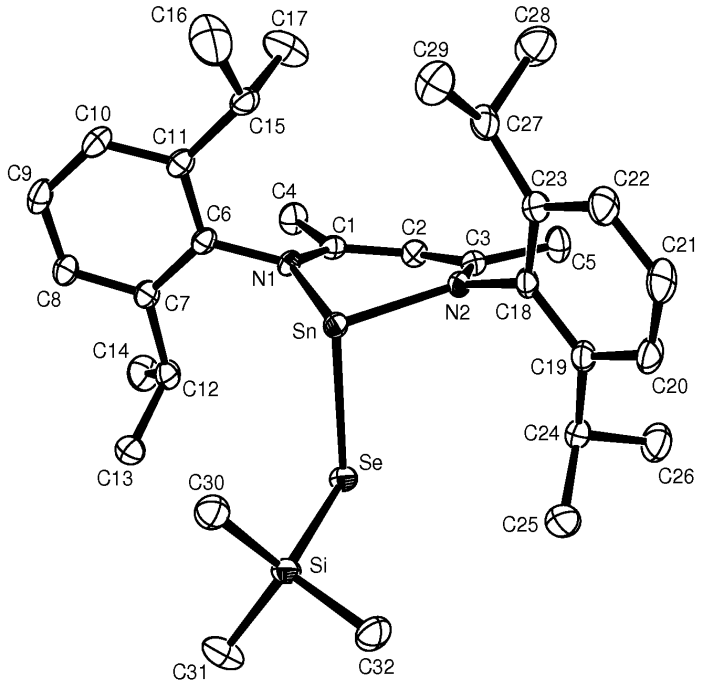
Figure S31. ORTEP diagram for [(BDI)SnSeSiMe$_3$] (**6**).